Stability of Hydrogenated Amorphous Carbon thin films for application in Electronic Devices

Sattam Alotaibi, Krishna Nama Manjunatha and Shashi Paul*

Emerging Technologies Research Centre, De Montfort University, The gateway, Leicester,LE18BH,United Kingdom

ABSTRACT

In this study, hydrogenated amorphous carbon (a-C:H) films are investigated for electronic applications as an insulating layer. a-C:H films were deposited using radio frequency-Plasma enhanced chemical vapour deposition (RF-PECVD) technique at room temperature. For the first time, the properties of a-C:H films as a function of annealing temperature is investigated, with a focus on their electrical and optical properties. This study shows that a-C:H films are stable up to 450°C. This investigation will facilitate the use of a-C:H films as an insulating layer where the semiconductor active layers are deposited at higher temperatures (e.g. amorphous silicon deposited around 300°C for thin film transistor TFTs). In addition to understanding the electrical and optical properties of annealed a-C:H films, we have further explored and studied its suitability in Flash-type memory devices. Various forms of diamond-like carbon are considered to have a high chemical resistance; no extensive data are available in the literature on this subject. The stability of a-C: H thin films with various reactive chemicals, commonly used in organic/printable electronic devices, is also investigated in this work. The findings may provide opportunities for adoption/integration of a-C:H in hybrid organic-inorganic electronic devices.

Keywords:

Diamond-like Carbon, Amorphous Carbon, Electronic Properties, PECVD, Insulator, Electronic Memory, stability of a-C:H

* Corresponding author. Tel: +44-116-207 8548. E-mail: spaul@dmu.ac.uk (Shashi Paul)

1. Introduction:

In recent years, hydrogenated amorphous carbon (a-C:H) films have attracted extensive attention because it endowed with a number of distinctive physical prosperities, such as high elastic modulus, extreme mechanical hardness, chemical inertness, and reduced surface roughness, thus making it a valuable unique material for a wide range of applications [1], [2], [3], [4], [5]. Of particular note are its exceptional properties including low-dielectric constant and wide optical bandgap, and these will facilitate the use of a-C:H as a semiconductor and/or low-k insulator thin film in almost all kinds of electronic applications [6], [7].

As an electrically insulating thin film plays a critical role in electronic devices, extensive research has been carried out in the fabrication of a thin film of both organic [8], [9] and inorganic [10]insulators such as polystyrene (PS) and diamond-like carbon (DLC). However, a-C:H film is an ideal thin film for electronic applications, as it demonstrates remarkable advantages compared with the other exploratory organic or inorganic insulating materials. This includes low fabrication cost, fabrication at room temperature, high mechanical flexibility and a good ability to adhere on to various substrates such as glass, plastic, silicon wafer (Si) and metal sheets/foils [5], [7], [11].

At present, electronic applications market is growing rapidly, and many electronic devices consist of several interlayers comprised of insulators, semiconductors and metals that are used in various architectures to fabricate an electronic device for a particular application [12]. These layers are often processed or deposited using the different fabrication processes in which few or all processes are performed in a vacuum, higher temperatures, under certain gaseous environment and low pressures. These thermodynamical variables have an outcome on the properties of thin films, but the deposition temperature can sustain a major effect on altering the properties of the deposited thin film. In the past two decades, a huge interest amongst researchers towards organic electronics has demonstrated good potential towards organic and/or hybrid organic-inorganic electronic devices as they offer some advantages over the inorganic material-based electronic devices. Hence, it is vital to understand the suitability of inorganic materials when used in conjunction with organic materials and such investigation is performed in this in-depth piece of work. The chemical inertness of diamond-like carbon encompasses opportunities to be exploited in various electronic devices as a protective coating, anticorrosion coating, Tribological applications, and dielectric and/or insulator layers [13], [14], [15].

Currently, the study of organic and flexible electronics has gained a momentum among electronic device community with an aim to create opportunities for the next generation electronic devices. In particular, non-volatile memory devices are being proposed and studies with the use of organic materials and/or hybrid structures [16], [17]. Amongst various organic memory devices, resistive and capacitive memory are studied the most due to the possibility of device miniaturization (scalable cross-bar architecture), appreciable operation speed including low energy consumption [18], [19]. Use of hybrid structures has improved stability by minimising the leakage current and reactivity of layers with the atmospheric gases. This is achieved by sandwiching the organic charge storage materials in between the dielectric insulating layers. However, deposition of organic materials over the underlying layers should not damage or cause undesired changes and, deteriorates the properties of underlying insulating layers. Therefore, insulating layer is required to be engineered to show extreme stability towards reactive gases and/or chemicals. And organic materials dispersed in the solvents and/or surface functionalised nanomaterials during the deposition process should not react with the underlying layers. As it is well known and established, in some cases to improve the dispersion of certain nanostructures in the polymer matrix, modification of their surface is achieved by anchoring functional groups that are subjected to acid treatment, which might cause undesired changes and deteriorate the underlying layers [16], [19]. Few exploratory memory devices are fabricated by others with the use of P3HT and PEDOT: PSS as a charge storage layer. Such chemicals are dispersed in aggressive reactive solvent, such as chloroform, dichlorobenzene or toluene. Therefore, it is an imperative for an insulating layer to be an inert to such aggressive solvents [19].

Once the thin film, in our case a-C:H, is deposited, it further goes through a number of processes; for example, heat treatment, exposure to plasma, exposure to chemicals, etc. In this work, we investigate the chemical resistance and temperature endurance of a-C:H thin films with an aim it to be exploited in electronic devices. Although, a number of studies have been reported on amorphous carbon [2], [7], [20], [21], [22], [23], [24], [25], to the best of our knowledge, there is no report on the investigation of post deposition heat treatment and exposure to commonly used organic solvents, in electronic industry, and the electrical and optical properties of a-C:H films deposited by RF-PECVD. Thus, this work will be the first study to focus on the understanding of stability, if any, of its properties as a function of annealing temperature and chemical resistance to commonly used organic solvents in semiconductor industries. This study will also help us to use a-C:H films with other

semiconductor/insulating materials which are deposited at elevated temperatures (e.g. amorphous hydrogenated silicon at 300°C). Moreover, a-C:H film was used as a dielectric film in metal-insulator-semiconductor (MIS) structures with/out selenium nanoparticles (SeNPs). These structures were fabricated to test the viability of a-C:H films in a Flash-type memory devices.

In order to understand the stability of a-C:H films, the films were characterised by using various techniques including, ellipsometry, depth profilometer, Fourier transform infrared (FTIR), Ultraviolet-Visible spectroscopy (UV-Vis), Raman spectroscopy, current-voltage (I-V) and capacitance-voltage (C-V) measurement techniques..

2. Experimental details:

2.1 Deposition of a-C:H thin films

The RF- PECVD technique is used to deposit a-C:H of 90±10 nm thin films. The thin films were deposited at room temperature using 110 sccm of argon (Ar) and 13 sccm of methane (CH_4) gases at a chamber pressure of 100 mTorr and DC self-bias voltage at -80V in Oxford-Plasma-Lab PECVD system. The deposition was performed for 10 minutes. The thermal stability of deposited films was investigated by post annealing at different of temperatures: 150°, 250°, 350°, 450° and 550°C in a vacuum chamber (45 mTorr base pressure) for 15 minute.

2.2 Characterisation and stability study of a-C:H thin films at various temperatures

a-C:H films were analysed using ellipsometry to determine the refractive index and film thickness. UV-Vis measurements were carried out on glass substrates (corning 2875-25) to determine optical gap and Urbach energy levels. FTIR spectroscopy is employed to calculate the relative hydrogen content in the a-C: H; for FTIR analyses, a-C: H films were deposited on a sapphire substrate. The film thickness was additionally measured with the use of profilometer. The Raman spectroscopy was carried out [26], on the a-C:H film deposited on glass substrates, in order to estimate sp^2 and sp^3 content within the deposited film. This measurement facilitated in understanding to observe the effect, if any, of annealing temperature on sp^2/sp^3 fraction in the thin films; a key parameter determines the electrical, mechanical and optical properties. For electrical measurements, two types of test structures

were prepared; Metal/a-C:H/Metal (MIM) and Metal/a-C:H/Si (MIS). The structures (namely the MIM and MIS) were fabricated in order to investigate the effect of post-annealing temperature on the electrical resistivity and dielectric constant of a-C:H films. The thermal evaporation was carried out at 1×10^{-6} Torr to deposit Aluminium (Al) (a metal used in the aforementioned structures).

2.3 Characterisation and stability study of a-C:H thin films subjected to various solvents

The reactivity or the chemical stability of a-C: H thin films towards commonly used organic solvents in the fabrication of organic and/or hybrid electronic devices is investigated by a simple non-destructive technique, by immersing the glass substrates coated with a-C: H film for a stipulated time, by determining their optical properties. a-C:H films were deposited on glass substrates that were sequentially cleaned by sonication in Decon-90, IPA and DI water. Although all the substrates were coated with a-C:H films under same PECVD deposition process, thickness varied by +/-10nm among the deposited samples that is due to the position of substrates within the chamber. Properties such as bandgap, transmittance, refractive index and thickness of amorphous hydrogenated carbon were measured with the use of ellipsometer, profilometer and UV-Vis spectrometer before and after immersion in various chosen solvents (listed in Fig. 13) for 15 minutes.

2.4 Fabrication of two-terminal memory device

The use of a-C:H film was investigated as an insulating layer in a two terminal memory device, which will provide insight and better understanding including potential to be used as an alternative insulating layer to replace those that are commonly used in COMS technology. To ensure reliable measurements, I-V measurements were conducted for the MIS devices, and only the devices showing a low leakage current (of less than 10 nA) were used in further analyses. C-V measurements. The C-V measurements were carried out in a shielded box with by applying ac bias of 50 mV at 1MHz.The MIS devices with/without selenium nanoparticles (SeNPs) were fabricated under the same deposition conditions on boron-doped (p-type) <100> silicon wafer substrates of resistivity 1-20 Ω-cm with Al ohmic back contact. The p-type silicon substrates were cleaned sequentially in Acetone, IPA, de-ionised water and dried with the use of N_2 gas. Then, SeNPs were deposited by selenium evaporation on the polished surface of the silicon substrate for 10 seconds in a thermal evaporator. Subsequently,

a-C:H was deposited as an insulating layer (45nm) under the same deposition conditions as mentioned in the previous section. Finally, Al top electrode was evaporated using a shadow mask as shown in Fig. 1**Error! Reference source not found.**.

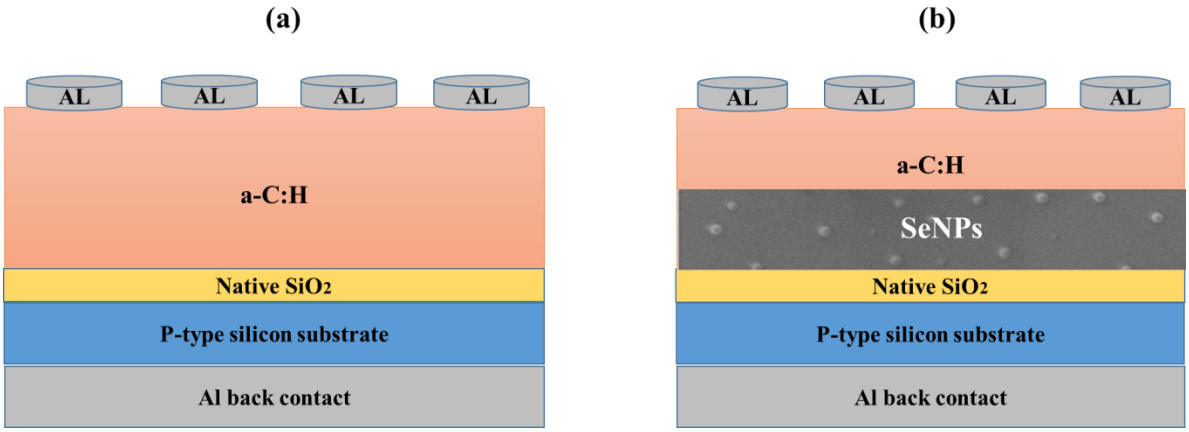

Fig. 1. **MIS device structures; (a) reference device without SeNPs; and (b) memory device containing S-NPs-10sec. These devices were used to understand the charging mechanism in SeNPs.**

3. Results and discussion:

3.1 Characteristics of a-C:H thin films

3.1.1 Thickness of a-C:H films:

Post-annealing of a-C:H films at higher temperatures may result in the change in physical and electrical properties which may result from the change in sp^2/sp^3 ratio. It is well known that in the electronic devices the thickness of the insulating layer, for example, in Thin Film Transistors (TFTs), plays an important role either to block the flow of electrons through it. The thickness of all annealed a-C:H films were measured and they were approximately 90±10nm, thus this result is acceptable in order to ensure accurate comparison of the relative sp^2 and sp^3 hybridisation and concentration of hydrogen in the deposited films. The thickness measurements carried out before and after annealing, the films have shown negligible variation in the thickness and the mean thickness was 90±10nm.

3.1.2 Dielectric constant (k) of a-C:H film:

A number of amorphous-carbon-based materials are investigated for their potential applications as low-k dielectrics [6], [25], [26], [27]. We also previously looked into the use

a-C: H films, equally low-k dielectrics and electrically insulating material, for electronic memory devices [10]. A number of researchers have investigated the dielectric constant of a-C:H, reported values for the dielectric constant (k) lies between 2.7 and 3.4 depending upon the deposition parameters [6], [27], [28], [29]. Interestingly, k of a-C:H films is a function of film thickness, and similar observation was seen in other published works [30].

In this work, the capacitance-voltage (C-V) characteristics of MIS structures (Al/a-C:H/Si^p/Al) were measured in order to estimate the k value of a-C:H film. As-deposited a-C:H film has dielectric constant k=2.6 and negligible change is observed up to temperature 450°C as shown in Fig. 2. This outcome is incoherent with the published work [28]. The k values of a-C:H decreases from 2.6 for as-deposited film to 2.5 when annealed at 450°C, this is a clear indication of the stability of films at temperatures below 450°C, it decreases to 2.2 at higher annealing temperatures >450°C. As a result of this, it is justifiable that a-C:H films show a transition at temperatures above 450°C, which is in accord with other published work [11], [23]. Annealing a-C:H films at temperatures above the transition temperature (450°C) leads to the graphitization conversion of C-C sp^3 bonded carbon to C-C sp^2 bonded carbon, and therefore leads to the release of compressive stress in the film [31]. Since the dielectric constant is proportional to stress or compactness in the film, the decreased value of k at a temperature above 450°C results from the stress release in the films or films are becoming less compact [1], [32].

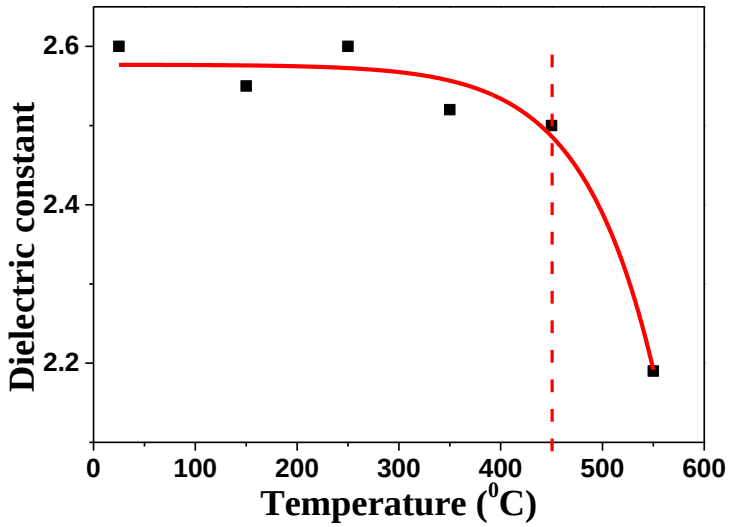

Fig. 2. Dielectric constant (k) of a-C:H vs. annealing temperatures. The dielectric constant is nearly similar up to temperature 450°C.

3.1.3 Hydrogen concentration in a-C:H film:

a-C:H film is a mixture of various allotropes of carbon; predominately comprised of sp^1 , sp^2 and sp^3, with 10-50% of hydrogen content. The hydrogen is required to stabilise the dangling bonds in a-C:H films. It determines the structure of the film, passivates the dangling bonds, and affects the compressive stress. As a consequence, H concentration in a-C:H films plays a significant role in determining both structural and physical attributes of the a-C:H films [7], [33], [34], [35].

The structures of molecules are characterised and detected with the use of FTIR spectroscopy. This technique is used to gain the information in regard to the absorption, and transmission of the infrared radiation in a-C:H films. In this case, it is useful for gathering information about the fraction of a-C:H; sp^3, sp^2 and sp^1 hybridised C-H bonds. It is well-known that FTIR spectroscopy cannot measure the absolute hydrogen content, but commonly used for the estimation of relative hydrogen concentration in the thin films.

In our previous study [36], the FTIR analysis is performed for a-C:H deposited on eight different substrates (Si^p, Si^{n+}, Si^n, glass corning 2875, alkali-free borosilicate glass corning 7059, gallium arsenide, quartz and sapphire), to see the effect of substrate in obtaining spectra. We observed that sapphire is the best substrate among all the selected substrates to perform FTIR analysis of DLC film in the wavenumber range of 2000 cm^{-1} and 3600 cm^{-1}. As a result of the aforementioned study, FTIR analysis was carried out of films deposited on Sapphire substrate.

As indicated in Fig. 3, a-C:H films deposited on sapphire substrates show a clear infrared absorption band centred at 2920cm^{-1}, which is attributed to CHx, where x has a value from 1 to 3. The specific combination of individual bands that contribute to the 2920 cm^{-1} of the band of these films, depends on the deposition conditions of the film, these results are in good agreement with the published works [1], [28].

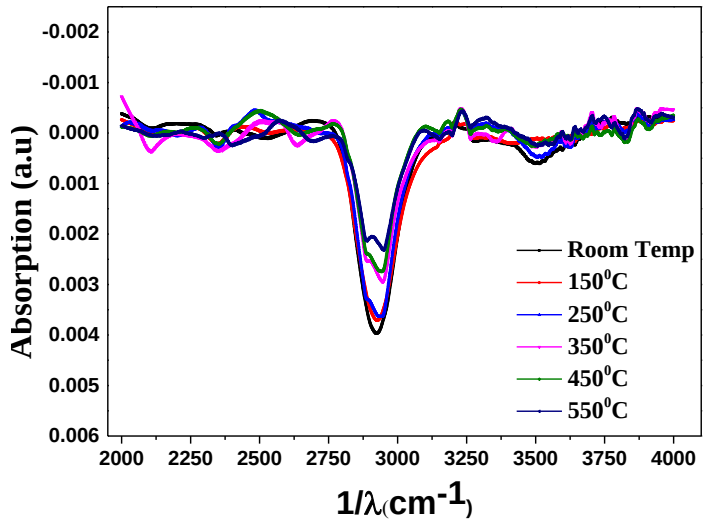

Fig. 3. FTIR absorption spectra of a-C:H film deposited on a sapphire substrate, at different annealing temperatures.

The fractional hydrogen content (C) was estimated by Equation (1) [1].

$C = A \int \frac{\alpha}{\omega} \, d\omega$ ….. Equation (1)

Where α is the absorption coefficient of a-C:H, ω is the wavenumber at which the absorption occurs and A is constant.

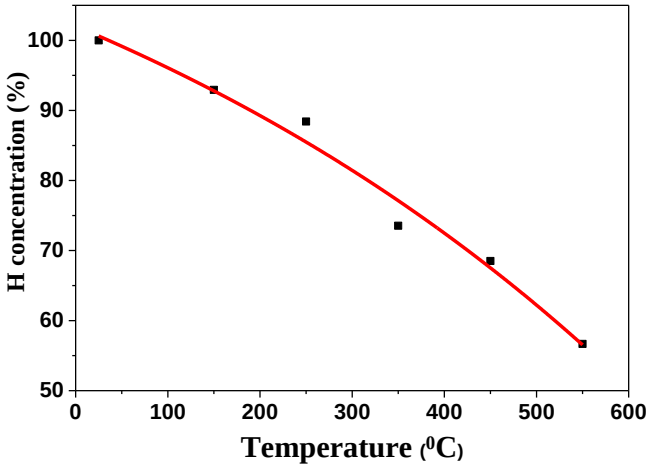

Fig. 4. Effect of annealing temperatures on the hydrogen content in the a-C:H films (Numerical to normalised relative concentation of a-C:H film deposited at room temperature). It is quite clear that the hydrogen content greatly reduced as a function of annealing temperature. This may cause an impending effect on both morphological and physical properties of the thin films.

The a-C:H film is metastable material and its structure is capable of changing towards graphite-like carbon by thermal activation [37]. Wild and Koidl [35]have suggested that the

transformation of a-C:H during annealing process occurs by the withdrawal of Hydrogen atom and hydrocarbon from the borders of the sp^2 dominated clusters and effusion through a network of boundaries decorated by hydrocarbons. The relative concentration of hydrogen is plotted in Fig. 4 as a function of annealing temperature; it is evident that there is a decrease in the relative hydrogen concentration with an increase in annealing temperature [22], [29], [37]. This could be imputed to the varieties in the relative fractions of the various phases of carbon or out-diffusion of hydrogen with higher annealing temperatures. It is also possible that at lower thermal activation up to 450°C, it is easy to eliminate any weakly bonded hydrogen from a-C:H films. The temperature above 450°C will lead to a damage of the structure into a mostly sp^2 bonded network [29]. As increasing hydrogen content in a-C: H deposited at low DC-bias is responsible for the increase in sp^3 fraction [3], higher annealing temperatures > 450°C shows an appreciable reduction in the hydrogen content that will result in the transition of sp^3 to sp^2 fraction due to loss of C-H bonds in sp^3 structures.

The index of refraction has been found to be dependent mainly on the hydrogen content of a-C:H films [29]. Fig. 5 shows the values of the index of refraction at different annealing temperatures, which increased from 1.910 for as-deposited film to 1.944 for films annealed up to 550°C, from Fig. 5 it is evident that the index of refraction is inversely proportional to hydrogen content. This kind of behaviour is similar to the work published by Grill [29]. Moreover, Fig. 5 shows a non-linear increase of the refraction index when the concentration of hydrogen in the a-C:H films reduce as a function of annealing temperature.

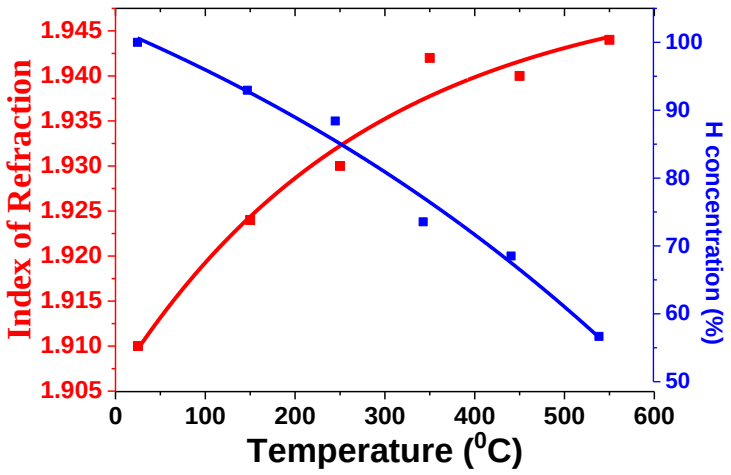

Fig. 5. The relationship between the hydrogen content in a-C:H films (Normalised relative concentration of a-C:H films deposited at -80V DC bias) and the Index of Refraction at various post-annealing temperatures.

3.1.4 Optical bandgap of a-C:H

The optical bandgap of the hydrogenated amorphous carbon material is an important parameter that serves to understand material properties suitable for specific applications. a-C:H film is a low mobility semiconductor, with an optical gap of 1-4eV [37]. The optical bandgap of a-C:H films are mainly determined by the fractional concentration of sp^2 bonds present in the films. As a consequence, there is a relationship between a sp^2 content and the bandgap of a-C:H film [7], [35], [37], [38].

The UV/Vis spectroscopy is the most commonly employed technique for determining the bandgap of amorphous semiconductor materials. The optical absorption edge of amorphous semiconductors is often analysed with the help of the Bandgap that is determined using Equation (2) [1]

$$E\alpha(E) = [B(E - E_T)]^2 \ldots. (2)$$

Here α(E) is the absorption coefficient at energy E , Tauc B parameter; E_T is the optical gap (Bandgap) of the a-C:H film and E is the energy of the photons used in the spectral analysis. Fig. 6 illustrates the marginal difference in the transmittance of UV-Vis spectra of a-C:H films annealed at different temperatures.

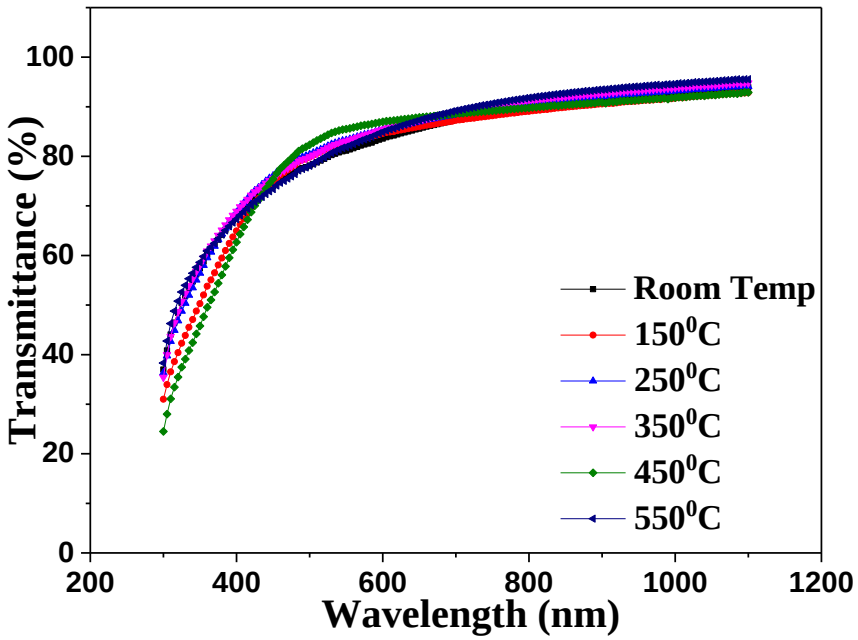

Fig. 6. Transmittance of UV/visible light through the a-C:H films deposited at same deposition conditions, and different annealing temperatures.

We count all the fits trustworthiness since the correlation coefficient is near to unity in all instances. The small change in the optical bandgap is observed with different annealing temperatures as shown in Fig. 7.

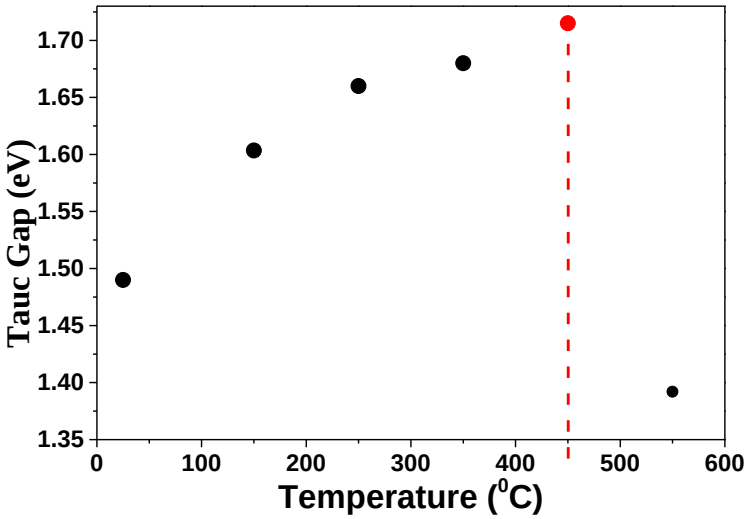

Fig. 7. Variation of Bandgap of a-C:H vs different annealing temperatures.

It is evident from Fig. 7 that the bandgap increases with the increase in annealing temperatures until the transition temperature (450°C), and then decreased for temperatures > 450°C, this observed trend is consistent with published work by others [11]. For a better understanding of variation in the Bandgap in Fig. 7, two regions are considered; region below and above the transition temperature. There is a slight increase in the bandgap as temperature increases from 1.49eV for as-deposited film to 1.72eV for film annealed at 450°C; this is attributed to a reduction in the size of sp^2 clusters due to loss of hydrogen bonds which is a consequence of the change within the structure to sp^2 bond network [37]. Interestingly, a reduction in hydrogen concentration and an increase in the bandgap of a-C: H film with an increase in temperature up to 450°C is observed. This corroborates the relation between H and sp^2 cluster size, which impact on E_T especially in thermal treatment lower than 450°C as reported [24], [39], [40]. On the other hand, bandgap decreased at region > 450°C, this can be attributed to changes in sp^3 to sp^2 clusters due to the loss of hydrogen bonds in sp^3 structures as mentioned earlier. Furthermore, the reduction in dielectric constant and Bandgap is observed at temperatures exceeding 450 °C. In overall, the size of sp^2 clusters indicates to a variation of the Bandgap (E_T) of a-C:H and both are inversely proportional to each other. Again, these results are consistent with published work [7], [23], [41].

In order to confirm the total change in the sp^2 content in a-C:H film, the Urbach energy (E_U) was calculated for a-C:H film annealed at different temperatures [42]. The E_U is evaluated as the inverse of the slope of In [α (E)] at the photon energy [25]. Fig. 8 provides additional evidence that the Bandgap is inversely correlated with sp^2 content in a-C:H film, where the decrease of the total sp^2 content with decreasing E_U from 1.56eV for as-deposited film to 1.39eV for film annealed at 450°C, leading to increased Bandgap. Thermal annealing above the transition temperature led to increase in E_U , thus, sp^2 sites has increased with the decrease in the bandgap. As mentioned earlier, the sp^2 content increased over transition temperature because of sp^3 is relaxed to sp^2 to release in stress (which is inherent in PECVD deposited films). However, for better understanding, characterisation of sp^2 concentration in a-C:H films with different annealing temperatures has to be established prior to making any judgement in the proposed work. Hence, Raman spectroscopy analysis is employed to understand the change in sp^2 contents as a function of the annealing temperature.

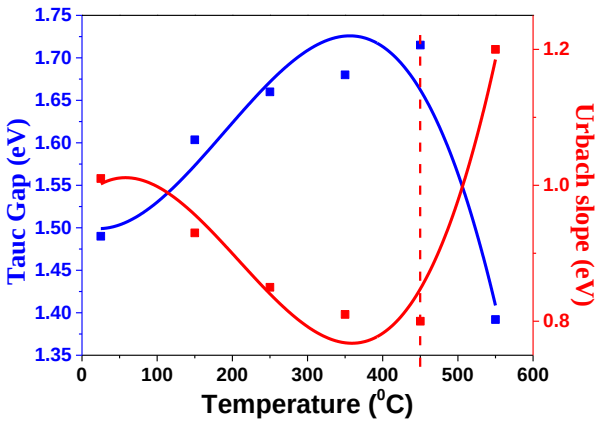

Fig. 8. Variation of Urbach energy and Bandgap for a-C:H films at different post-annealing temperatures.

3.1.5 Characterisation of sp^2 content in a-C:H film:

Raman spectroscopy is the most powerful technique to confirm the effect of annealing temperatures on sp^2 cluster size in a-C:H films. The Raman spectra collected from a-C:H films are shown in Fig. 9(a). The film has shown a band at 1510±20cm^{-1} which is consistent with the literature [43], [44]. It is noticeable from Fig. 9(b) that there is a shift in the bands towards the shorter wavelengths from 1510cm^{-1} to 1524cm^{-1} with an increase in temperatures up to 450°C, then slight decrease at a temperature above 450°C. This is possibly due to a basic restructuring of bonds in the a-C:H films, as a consequence of annealing films at higher temperatures. However, the change in the structural properties of a-C:H film is understood by D and G bands in the Raman Spectra [26], [32], [40], [41]. Spectrum data between 1000 and

2000 cm^{-1} were de-convoluted into the D and G bands, characteristic of a-C:H film annealed at a certain temperature. Optimum fitting was done by permitting all the fit parameters, peak positions and widths, to vary.

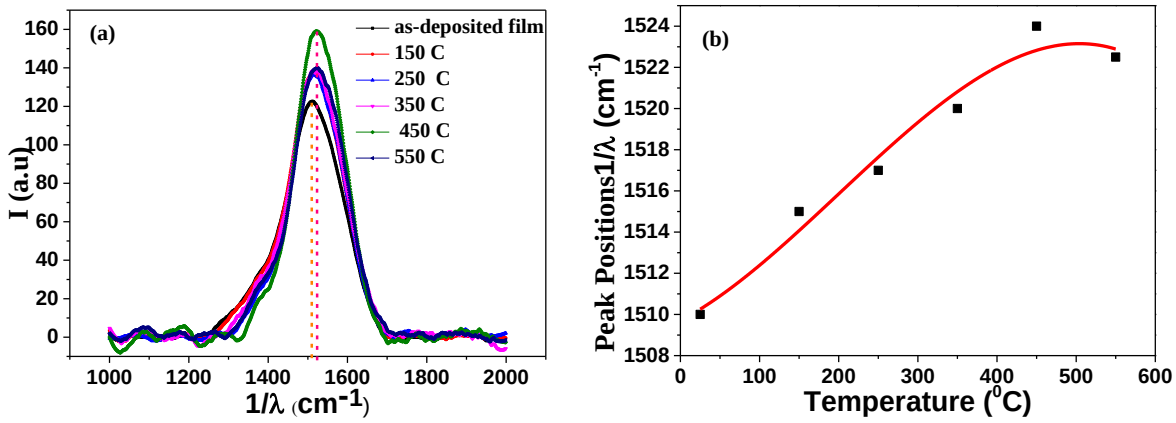

Fig. 9. (a) Shows Raman Spectra of a-C:H film on a glass substrate at various annealing temperatures, (b) Shows the band positions at different temperatures.

The Raman spectra of a-C:H films are dominated by a G band around 1500 cm^{-1} due to sp^2 bond stretching and a D band around 1360 cm^{-1} as a result of finite aromatic sheets [24]. Moreover, Wagner et al. [44]proposed that the Raman spectra of a-C:H film does have a D-band shoulder, indicating some aromatic or benzene clusters incorporated in a-C:H film. Fig. 10 illustrates the typical and de-convoluted Raman spectra of disordered graphite of as-deposited film Fig. 10(a), and annealed film at 550°C Fig. 10(b). Broadly speaking, the two-curve Gaussian function is enough to analyse the single Raman spectra into two bands.

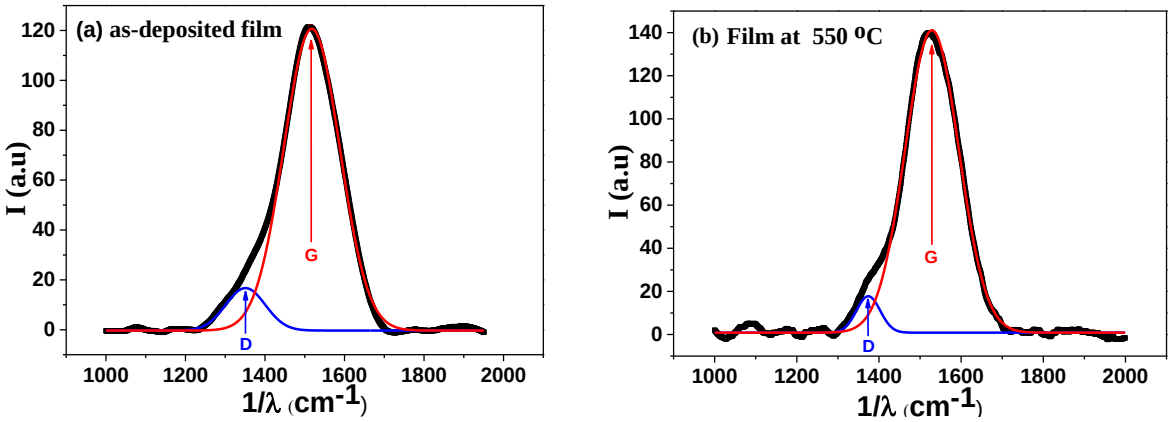

Fig. 10. Shows the D and G peaks are de-convoluted by Gaussian peak-fitting in Raman Spectra of a-C:H. (a) the as-deposited film, and (b) At 550°C.

However, in order to estimate the sp^2 bond concentration, the ratio of the intensities/ area of the bands should be calculated as depicted in Fig. 11(a) and Fig. 11(b) respectively, from these

figures we can confirm that both ratios of the intensity and the ratio of the area of D and G peaks are quite similar, as a result of that it is adequate to study and analyse either of them.

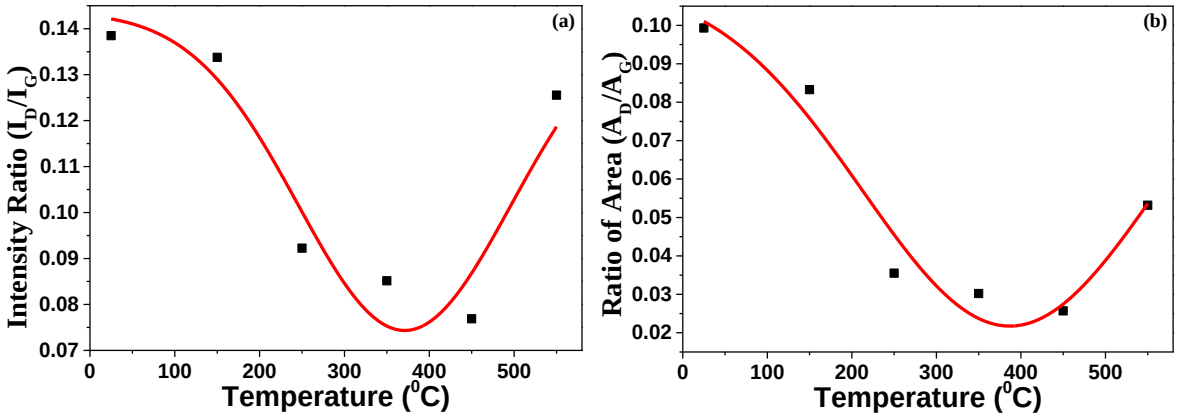

Fig. 11. (a) I_D/I_G ratio, (b) A_D/A_G ratio of our a-C:H films, at different annealing temperatures.

It is understood from the Fig. 11(a) that the I_D/I_G ratio of a-C:H decreased with the increase in annealing temperatures until the transition temp at 450°C, and then rapidly increased. Such a change in the intensity ratio (I_D/I_G) can be attributed to the compositional change in the film [1], [21], [45]. The I_D/I_G ratio is a measure of the fractional concentration of sp^2 bonds in a-C:H film, therefore, the size of the sp^2 phase organised in the rings decreased with annealing temperature up to 450°C, and at a higher annealing temperature > 450°C; the a-C:H film begins gradual graphitization because of the higher fractional content of sp^2 bonds in the film [7], [21], [33], [39]. However, it's worth to mention that content of sp^2 characterised by Urbach energy derived from UV-Vis spectra and I_D/I_G ratio derived from Raman spectra agree with each other.

3.1.6 Electrical measurements

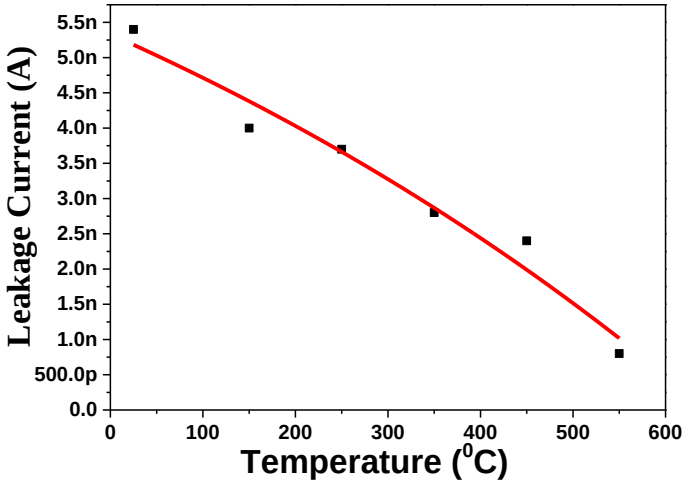

Fig. 12. Variation in the leakage current at 5V as a function of annealing temperature.

Current-Voltage measurements were carried out, to understand the electrical properties (namely the leakage current) as a function of annealing temperature. Fig. 12 shows that there is a negligible reduction in the leakage current with an increase in the annealing temperature. The possible explanation could be suggested based on the bandgap widening at elevated temperature. Further investigation is underway to pinpoint the underlying science.

3.2 Stability of a-C:H films

During the deposition process involved in the fabrication of electronic devices that consist of organic layers containing reactive solvents may cause damage to underneath layers. Hence, it is important to study the stability of insulators (a-C:H used in this work) to these reactive solvents that are commonly used in organic materials either dispersed or dissolved. This Study has already discussed about the stability of a-C:H thin films towards temperatures up to 450^{o}C that is also promising to be exploited in CMOS based architectures/devices [17]. In this section chemical resistance of a-C:H coated substrates towards reactive chemicals is studied by measuring few properties before and after immersing in the range of solvents as listed in **Fig. 13**. Such a study will provide better insights about stability towards commonly used solvents expanding opportunities of exploiting a-C:H thin films in hybrid organic memory devices. This work describes room temperature deposition of a-C:H thin films that additionally provided opportunities to select flexible plastic substrates.

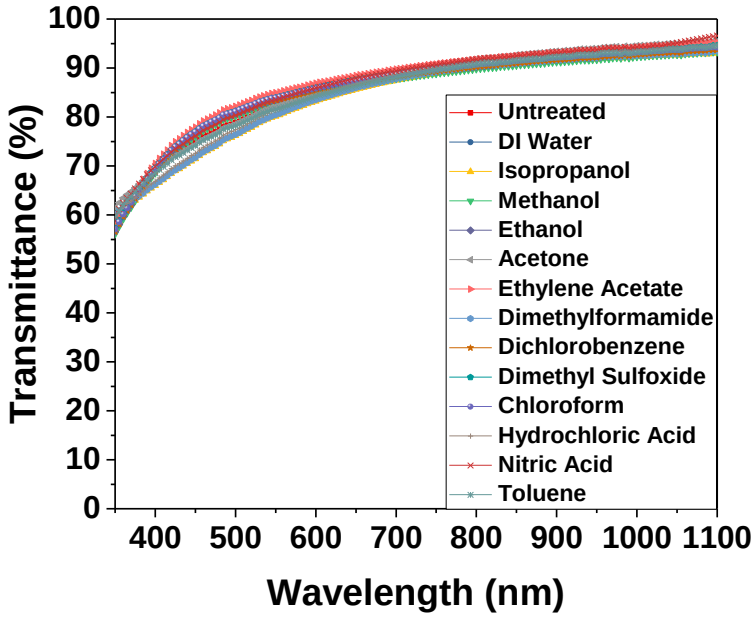

Fig. 13. Transmittance data of a-C:H thin films coated on glass substrates immersed in various solvents for 15 min.

Table 1. Stability study of a-C:H film in with different solvents by measuring the key properties bandgap, thickness and RI before and after treatment.

Solvent	Bandgap (eV)	Bandgap (eV)	Thickness (nm)		RI	
	Before	After	Before	After	Before	After
Reference (Untreated)	1.48	1.48	91	91	1.935	1.935
DI Water	1.48	1.48	95	95	1.932	1.932
Isopropanol	1.48	1.48	93	93	1.928	1.928
Methanol	1.56	1.56	84	84	1.912	1.914
Ethanol	1.48	1.48	86	86	1.916	1.916
Acetone	1.48	1.48	92	92	1.931	1.936
Ethylene Acetate	1.52	1.52	85	85	1.911	1.911
Dimethylformamide	1.57	1.57	87	87	1.915	1.912
Dichlorobenzene	1.52	1.52	95	95	1.930	1.930
Dimethyl Sulfoxide	1.53	1.53	93	93	1.931	1.931
Chloroform	1.52	1.52	91	91	1.932	1.932
Hydrochloric Acid	1.52	1.52	88	88	1.916	1.918
Nitric Acid	1.53	1.53	85	85	1.925	1.923
Toluene	1.57	1.57	60	60	1.913	1.913

To determine chemical resistance of a-C:H thin films in the selected solvents (listed in Table1), properties such as transmittance, bandgap, refractive Index and thickness of the films are measured before and after immersing the a-C:H coated substrates in the chosen solvents (**Fig. 13**). It is worth to mention that a-C:H thin film coated samples did not have same thickness value for all the films. However, each individual sample was selectively measured to determine the properties before and after immersing in the chosen solvent. It is evident from the Table 1. that the measured properties showed either no change or negligible change. This further provides strong evidence for extreme stability of a-C:H thin films when exposed or in contact with the solvents described/used in this work [46]. This suggests that a-C:H thin films are expected to be chemically unreactive like diamond. It is worth to mention that glass substrates does not react to the solvents used in this work, hence pin-holes present within the film, if any, may not lead to further damage in the films such as peeling off issues. A similar observation was performed for PECVD coated a-C:H films on aluminium substrates that peeled due to the acids reacting at the surface of underlying aluminium that penetrated through the pin-holes present in the films [47]. a-C:H films deposited by PECVD technique provide conformal coating and may have pin-holes if the surface of substrate on which it is coated is not uniform. It is possible to detect defects in the a-C:H film coated on metal substrates by dropping acids such as HCL, that could lead to quick test in industries to claim conformal coating. In this work chemical resistance is measured for 15 minutes

considering that any solvent based organic layer coating techniques such as spin coating, wire-wound coating, dip coating and doctor blade coating does not exceed above mentioned time period. Several other coating techniques such as Langmuir-Blodgett requires an enhanced time period for the deposition of material, it is recommended that inertness of a-C:H to be tested for the duration that any coating technique is performed. Additionally, a-C: H films coated on Si wafers were also investigated as described above that shows similar conclusions confirming the inertness of a-C:H films. It is equally important to maintain cleanliness of the substrate's surface and deposition process that might otherwise lead to the pin-holes and defects in the films. Presence of pin-holes and defects will lead to penetration of solvents that might either react with the substrate further causing peeling related issues in the film, more investigations are required to corroborate these findings. Such a stable film is promising to be used in any hybrid organic electronic devices including two terminal memory devices discussed here. Hence, a-C:H thin films deposited in this work show excellent chemical stability and CMOS process compatibility, possibly reducing operation current/voltage, which is promising for next generation information storage in flexible systems.

3.3 Application of a-C:H films in electronic memory

First, it was necessary to ensure that the hysteresis attained by incorporating selenium nanoparticles in the MIS device was in fact due to charge storage in SeNPs, and not because of a-C:H film containing electronic defect states. Therefore, a C-V measurement was carried out on the MIS reference device without SeNPs, as shown in **Fig. 14**. a negligible hysteresis was observed for the reference device, with only an insignificant flat band voltage shift of less than 0.2v for a +10/-10v sweep range at 1MHz. Negligible hysteresis observed in the C-V curve is indicative of the absence of a charge trapped/stored in the dielectric layer (a-C:H). It was also seen that the C-V hysteresis loop for the device containing a dielectric layer (a-C:H) showed a gradual increase in the curve from inversion to accumulation region. This means the switching between two different capacitance states (low and high) will be slower. The non-appearance or insignificant existence of the C-V hysteresis loop in the reference device suggests that negligible charge was stored or retained in this device. Similar results were observed with different MIS devices investigated for insulators as a reference device [48], [49], [50].

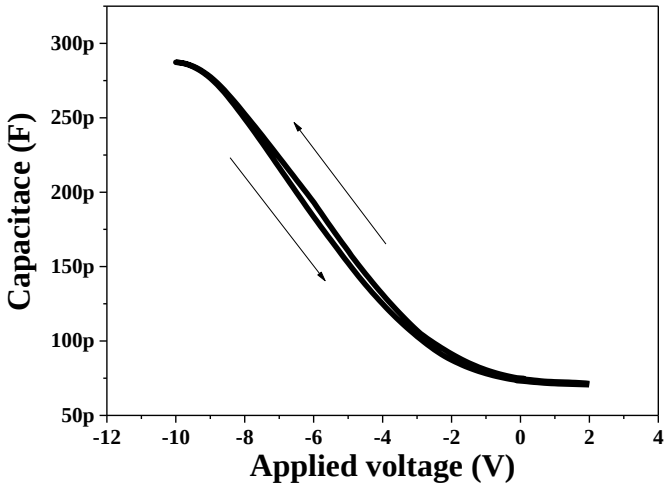

Fig. 14. C-V characteristics measured for voltage sweep from +10V to -10V that applied to the top contact of the MIS capacitor without SeNPs (reference device). The arrows indicate the anticlockwise direction of the C-V hysteresis loops; the hysteresis loop was very tiny (neglected) due to no charge trap or store in this structure.

Conversely, in **Fig. 15**, the MIS device containing SeNPs exhibited large hysteresis loops. These C-V hysteresis loops were detected to be moving in anticlockwise direction, as the sweep voltages were decreased from the inversion region (positive applied voltage axis) to the accumulation region (negative applied voltage axis), and back to inversion at a higher frequency (1MHz) and 0.5s time delay. The anticlockwise hysteresis loop for MIS structures observed in a p-type silicon substrate is usually an indication of charges stored or trapped in nanoparticles (in our case, SeNPs) and injected through a tunnelling oxide layer (SiO_2) [49]. Moreover, it was also seen that the width of the C-V hysteresis loop increased with an increase in the sweep voltage. Thus, the flat band voltage shift between the forward (inversion to accumulation) and backward (accumulation to inversion) sweep can be calculated from the C-V hysteresis width. The flat band voltage and total area of hysteresis was found to increase almost in line with the sweep voltage range on the MIS device. This is expected as more charges injected and stored within the active layer by increasing the sweep voltage, similar results were reported by other researchers [51]. The C-V hysteresis direction can offer information in regard to the charges are being injected through the blocking layer (a-C:H film) or through the tunnelling layer (Native SiO_2). If the holes were being stored/trapped, the C-V hysteresis will be positioned in the negative side of the applied voltage axis. Moreover, if clockwise C-V curve is observed, then the holes are being stored/trapped under a positive gate voltage which requires the holes being tunnelled through the a-C:H film. On the other hand, if the C-V curve is anticlockwise then the holes have to be

tunnelled under a negative gate voltage, hence are being tunnelled through SiO_2. The consequence of electrons being stored/trapped resulting in the C-V hysteresis being positioned in the positive side of the applied voltage axis. Clockwise direction in the hysteresis indicates that the electrons are being under negative gate bias, hence tunnelling is through the a-C:H film. Conversely, if the hysteresis loop is obtained in anticlockwise direction, then the electrons have to be tunnelled under positive gate bias [52], [53]. MIS device fabricated in this work, showed C-V hysteresis window to be 2.79V at a +10/-10 V sweep range, as shown in **Fig. 15**.

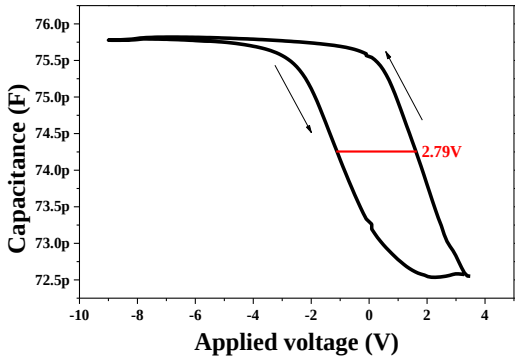

Fig. 15. C-V characteristics measured for voltage sweep +/-10V that applied to the top contact of the MIS structure containing SeNPs (MIS memory device). In the C-V hysteresis, the arrows indicate the anticlockwise direction. The memory window and flat band shift high increased compared to MIS reference, because of the existence of storage elements (SeNPs).

4. Conclusion:

In brief, the electrical and optical properties of a-C:H films are stable up to the transition temperature (450 $^{\circ}$C). However, electrical and optical properties of the a-C:H films are affected beyond 450 $^{\circ}$C due to loss of hydrogen from sp^2 clusters and/or conversion of clusters from sp^3 to sp^2 hybridisation. In-depth investigation is performed with an aid of several characterisations techniques detailed in this work to provide better understanding of the instability beyond transition temperature. Such a stable film will be an added benefit for integration of a-C:H films deposited at room temperature in the C-MOS technology. Additionally, a-C:H films introduced to several aggressive reactive chemicals show promising results which extreme stability that provides opportunities for integration in organic electronic devices. a-C:H films are possible to be used as an insulating layer in existing and futuristic electronic devices such as memory devices discussed here. This work has shown first proof of concept of flash memory device that incorporates a-C:H film as a

dielectric insulating film. It is worth to mention that all the layers used in the fabrication of memory device are deposited by keeping the substrate at a room temperature without any intentional heating. This study, for the first time, shows that there is no effect of commonly used organic solvents on the optical properties of a-C:H.

Acknowledgment:

The first author would like to thank Taif University in Saudi Arabia for sponsoring his PhD studies at the Emerging Technologies Research Centre, De Montfort University, in the United Kingdom. The author (SP) would like to thank EPSRC (Grant #EP/E047785/1) for supporting this work.

References

[1] S. Paul, *Growth, characterisation and electronic applications of amorphous hydrogenated carbon*, De Montfort University, Leicester, 2000.

[2] J. Robertson, *Improving the properties of diamond-like carbon*, 2003Available from: http://www.sciencedirect.com/science/article/pii/S0925963503000062.

[3] Y. Chen, T. Ma, P. Zhu, D. Yue, Y. Hu, Z. Chen and H. Wang, *Growth mechanism of hydrogenated amorphous carbon films: Molecular dynamics simulations*, 2014Available from: http://www.sciencedirect.com/science/article/pii/S0257897214006720.

[4] M. Noborisaka, R. Horikoshi, S. Nagashima, A. Shirakura and T. Suzuki, *Hardness and surface roughness of hydrogenated amorphous carbon-based films synthesized by atmospheric pressure-plasma enhanced chemical vapor deposition at low temperature*, 2013Available from: http://www.sciencedirect.com/science/article/pii/S0040609012015623.

[5] S. Paul and F.J. Clough, *A reliability of different metal contacts with amorphous carbon*, 2002Available from: http://www.sciencedirect.com/science/article/pii/S0026271401001330.

[6] A. Grill, V. Patel, K.L. Saenger, C. Jahnes, S.A. Cohen, A.G. Schrott, D.C. Edelstein and J.R. Paraszczak, *Diamondlike carbon materials as low-k dielectrics for multilevel interconnects in ulsi*, Cambridge University Press, 1996Available from: https://www.cambridge.org/core/article/diamondlike-carbon-materials-as-lowk-dielectrics-for-multilevel-interconnects-in-ulsi/C151DE56D764DDE2C5B32A4A030E0618[Accessed 2018/09/17].

[7] S. Pisana, S.K. O'Leary and S. Zukotynski, *Optical properties of hydrogenated amorphous carbon thin films prepared by dc saddle field plasma-enhanced chemical vapor deposition*, 2005Available from: http://www.sciencedirect.com/science/article/pii/S0022309305000888.

[8] J. Ouyang, C. Chu, R.J. Tseng, A. Prakash and Y. Yang, *Organic memory device fabricated through solution processing*, IEEE, 2005.

[9] J. Ouyang, C. Chu, D. Sieves and Y. Yang, *Electric-field-induced charge transfer between gold nanoparticle and capping 2-naphthalenethiol and organic memory cells*, American Institute of Physics, 2005Available from: https://doi.org/10.1063/1.1887819.

[10] S. Alotaibi, N. Gabrielyan and S. Paul, *Two terminal non-volatile memory devices using diamond-like carbon and silicon nanostructures*, Trans Tech Publications, 2014Available from: https://www.scientific.net/AST.95.100.

[11] F.W. Smith, *Optical constants of a hydrogenated amorphous carbon film*, American Institute of Physics, 1984Available from: https://doi.org/10.1063/1.333135.

[12] J. Ouyang, C. Chu, C.R. Szmanda, L. Ma and Y. Yang, *Programmable polymer thin film and non-volatile memory device*, Nature Publishing Group, 2004Available from: http://dx.doi.org/10.1038/nmat1269.

[13] H. Moriguchi, H. Ohara and M. Tsujioka, *History and applications of diamond-like carbon manufacturing processes*, 2016.

[14] D.A. Outka, W.L. Hsu, K. Phillips, D.R. Boehme, N. Yang, D.K. Ottesen, H.A. Johnsen, W.M. Clift and T.J. Headley, *Compilation of diamond-like carbon properties for barriers and hard coatings*

no title, 1994.

[15] Al Mahmud, K. A. H., M.A. Kalam, H.H. Masjuki, H.M. Mobarak and N.W.M. Zulkifli, *An updated overview of diamond-like carbon coating in tribology*, Taylor & Francis, 2015Available from: https://doi.org/10.1080/10408436.2014.940441.

[16] T.W. Kim, Y. Yang, F. Li and W.L. Kwan, *Electrical memory devices based on inorganic/organic nanocomposites*, Nature Publishing Group, 2012.

[17] R. Huang, Y. Cai, Y. Liu, W. Bai, Y. Kuang and Y. Wang, *Resistive switching in organic memory devices for flexible applications*, IEEE, 2014.

[18] D. Prime and S. Paul, *Overview of organic memory devices*, 2009Available from: http://rsta.royalsocietypublishing.org/content/367/1905/4141.abstract.

[19] I. Rosales-Gallegos, J.A. Ávila-Niño, D. Hérnandez-Arriaga, M. Reyes-Reyes and R. López-Sandoval, *Flexible rewritable organic memory devices using nitrogen-doped CNTs/PEDOT:PSS composites*, 2017Available from: http://www.sciencedirect.com/science/article/pii/S1566119917301179.

[20] M. Theye and V. Paret, *Spatial organization of the sp2-hybridized carbon atoms and electronic density of states of hydrogenated amorphous carbon films*, 2002Available from: http://www.sciencedirect.com/science/article/pii/S0008622301002913.

[21] T. FC and T. SL, *Correlation between ID/ IG ratio from visible raman spectra and sp2/sp3 ratio from XPS spectra of annealed hydrogenated DLC film*, The Japan Institute of Metals and Materials, 2006.

[22] P. Yang, S.C.H. Kwok, R.K.Y. Fu, Y.X. Leng, J. Wang, G.J. Wan, N. Huang, Y. Leng and P.K. Chu, *Structure and properties of annealed amorphous hydrogenated carbon (a-C:H) films for biomedical applications*, 2004Available from: http://www.sciencedirect.com/science/article/pii/S0257897203009058.

[23] X.-. Tang, J. Weber, S.N. Mikhailov, C. Müller, W. Hänni and H.E. Hintermann, *Structure stability of hydrogenated amorphous carbon film during thermal annealing*, 1995Available from: http://www.sciencedirect.com/science/article/pii/0022309395006729.

[24] J. Robertson, *Structural models of a-C and a-C:H*, 1995Available from: http://www.sciencedirect.com/science/article/pii/0925963594052646.

[25] G. Fanchini and A. Tagliaferro, *Disorder and urbach energy in hydrogenated amorphous carbon: A phenomenological model*, American Institute of Physics, 2004Available from: https://doi.org/10.1063/1.1776633.

[26] J. Schwan, S. Ulrich, V. Batori, H. Ehrhardt and S.R.P. Silva, *Raman spectroscopy on amorphous carbon films*, American Institute of Physics, 1996Available from: https://doi.org/10.1063/1.362745.

[27] A. Grill, V. Patel and C. Jahnes, *Novel low k dielectrics based on diamondlike carbon materials*, The Electrochemical Society, 1998.

[28] A. Grill, *Amorphous carbon based materials as the interconnect dielectric in ULSI chips*, 2001Available from: http://www.sciencedirect.com/science/article/pii/S0925963500004738.

[29] A. Grill, *Electrical and optical properties of diamond-like carbon*, 1999Available from: http://www.sciencedirect.com/science/article/pii/S0040609099005167.

[30] Katsuhiro Yokota and Yuuya Miyoshi and, Masaki Saoyama, *Very low dielectric constants of diamond-like carbon films deposited on ground electrode by plasma-enhanced chemical vapor deposition*, 2006Available from: http://stacks.iop.org/1347-4065/45/i=2R/a=860.

[31] N.W. Khun and E. Liu, *Effects of platinum content on tribological properties of platinum/nitrogen doped diamond-like carbon thin films deposited via magnetron sputtering*, 2014Available from: https://doi.org/10.1007/s40544-014-0040-8.

[32] A.C. Ferrari and J. Robertson, *Interpretation of raman spectra of disordered and amorphous carbon*, APS, 2000.

[33] C. Casiraghi, A.C. Ferrari and J. Robertson, *Raman spectroscopy of hydrogenated amorphous carbons*, American Physical Society, 2005Available from: https://link.aps.org/doi/10.1103/PhysRevB.72.085401.

[34] S. Paul, *Substrate selection for the infra-red analysis in amorphous hydrogenated carbon films*, Elsevier, 2007.

[35] C. Casiraghi, J. Robertson and A.C. Ferrari, *Diamond-like carbon for data and beer storage*, 2007Available from: http://www.sciencedirect.com/science/article/pii/S1369702106717916.

[36] S. Alotaibi, K. Nama and S. Paul, *A study in pursuit of precise substrate selection for infrared spectroscopy analysis of diamond-like carbon films*, World Scientific, 2016.

[37] A. Grill, *Diamond-like carbon: State of the art*, 1999Available from: http://www.sciencedirect.com/science/article/pii/S0925963598002623.

[38] Gielen, J. W. A. M., P.R.M. Kleuskens, d.S. van, L.J. van Ijzendoorn, D.C. Schram, E.H.A. Dekempeneer and J. Meneve, *Optical and mechanical properties of plasma‐beam‐deposited amorphous hydrogenated carbon*, American Institute of Physics, 1996Available from: https://doi.org/10.1063/1.363567.

[39] Z. Tang, Z.J. Zhang, K. Narumi, Y. Xu, H. Naramoto, S. Nagai and K. Miyashita, *Effect of mass-selected ion species on structure and properties of diamond-like carbon films*, American Institute of Physics, 2001Available from: https://aip.scitation.org/doi/abs/10.1063/1.1333739.

[40] C. Wild and P. Koidl, *Thermal gas effusion from hydrogenated amorphous carbon films*, American Institute of Physics, 1987Available from: https://doi.org/10.1063/1.98617.

[41] J. Robertson and E.P. O'reilly, *Electronic and atomic structure of amorphous carbon*, APS, 1987.

[42] G. Fanchini and A. Tagliaferro, *A new interpretation of the urbach energy in amorphous carbon films*, 2004Available from: http://www.sciencedirect.com/science/article/pii/S0925963503004837.

[43] A.A. Ogwu, R.W. Lamberton, S. Morley, P. Maguire and J. McLaughlin, *Characterisation of thermally annealed diamond like carbon (DLC) and silicon modified DLC films by raman*

spectroscopy, 1999Available from: http://www.sciencedirect.com/science/article/pii/S0921452699001386.

[44] J. Wagner, M. Ramsteiner, C. Wild and P. Koidl, *Resonant raman scattering of amorphous carbon and polycrystalline diamond films*, APS, 1989.

[45] D. Franta, V. Buršíková, I. Ohlídal, L. Zajíčková and P. St′ahel, *Thermal stability of the optical properties of plasma deposited diamond-like carbon thin films*, 2005Available from: http://www.sciencedirect.com/science/article/pii/S0925963505003663.

[46] C.A. Brookes and E.J. Brookes, *Diamond in perspective: A review of mechanical properties of natural diamond*, Elsevier, 1991.

[47] D.A. Outka, W.L. Hsu, K. Phillips, D.R. Boehme, N. Yang, D.K. Ottesen, H.A. Johnsen, W.M. Clift and T.J. Headley, *Compilation of diamond-like carbon properties for barriers and hard coatings*, Sandia National Labs., Livermore, CA (United States); Sandia National Labs., Albuquerque, NM (United States), 1994.

[48] T. Mih Atta, *A novel low-temperature growth method of silicon structures and application in flash memory*, De Montfort University, Leicester, 2011.

[49] M.F. Mabrook, A.S. Jombert, S.E. Machin, C. Pearson, D. Kolb, K.S. Coleman, D.A. Zeze and M.C. Petty, *Memory effects in MIS structures based on silicon and polymethylmethacrylate with nanoparticle charge-storage elements*, 2009Available from: http://www.sciencedirect.com/science/article/pii/S0921510708003656.

[50] M.F. Mabrook, C. Pearson, D. Kolb, D.A. Zeze and M.C. Petty, *Memory effects in hybrid silicon-metallic nanoparticle-organic thin film structures*, 2008Available from: http://www.sciencedirect.com/science/article/pii/S1566119908001055.

[51] S. Fakher, R. Nejm, A. Ayesh, A. Al-Ghaferi, D. Zeze and M. Mabrook, *Single-walled carbon-nanotubes-based organic memory structures*, Multidisciplinary Digital Publishing Institute, 2016.

[52] V. Mikhelashvili, Y. Shneider, B. Meyler, G. Atiya, S. Yofis, T. Cohen-Hyams, W.D. Kaplan, M. Lisiansky, Y. Roizin and J. Salzman, *Non-volatile memory transistor based on pt nanocrystals with negative differencial resistance*, AIP, 2012.

[53] D. Prime C, *Switching mechanisms, electrical characterisation and fabrication of nanoparticle based non-volatile polymer memory devices*, De Montfort University, Leicester, 2010.

Supporting Information for

Stability of Hydrogenated Amorphous Carbon thin films for applications in Electronic Devices

Sattam Alotaibi, Krishna Nama Manjunatha and Shashi Paul*

Emerging Technologies Research Centre, De Montfort University, The gateway, Leicester,LE18BH,United Kingdom

***Corresponding authors**:

E-mail address: spaul@dmu.ac.uk (Shashi Paul)

1. **Thickness measurements of a-C:H films**

a-C:H films thickness was measured by profilometer and also verified by ellipsometry as shown in Fig.S1**Error! Reference source not found.**. It is quite clear that variation in thickness with different annealing temperatures is negligible and it can be neglected, and thus the mean thickness is 90±10nm.

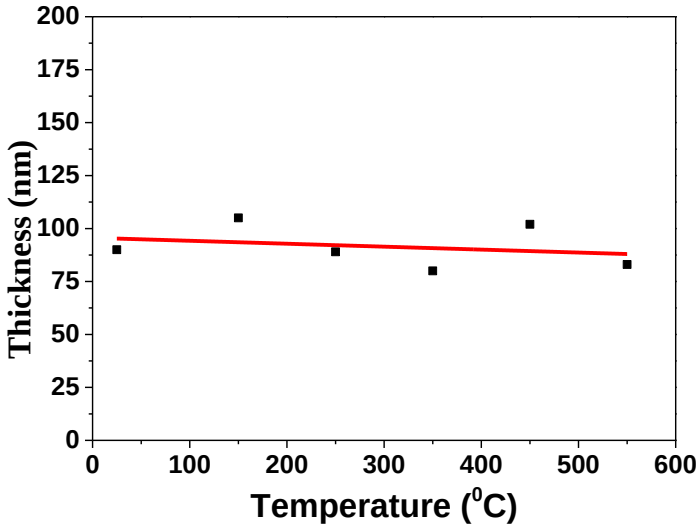

Fig.S1 Variation of the thickness of the a-C: H films deposited under similar process conditions subjected to different post-annealing temperatures.

2. **Determination of Bandgap by curve fitting method.**

To determine the Bandgap, we plotted experimentally collected data as depicted in and fitted equation (2) to the data. The Bandgap was gathered from the parameters in this fit, using Equation (2). We count all the fits trustworthiness since the correlation coefficient is near to unity in all instances. **Error! Reference source not found.**

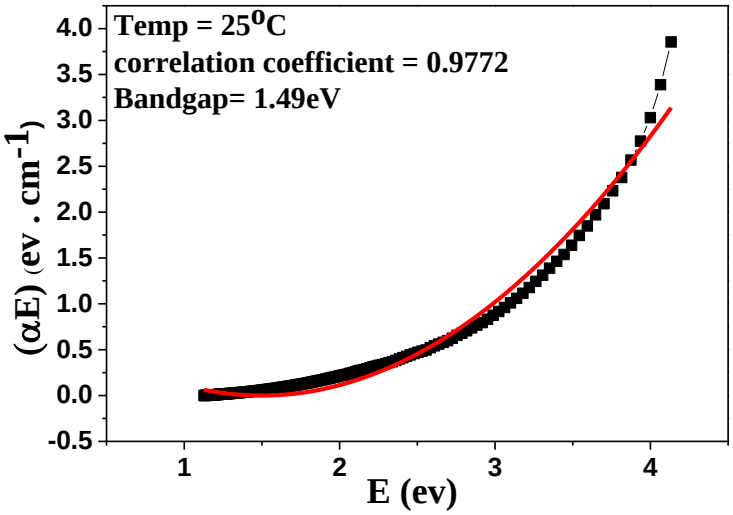

Fig.S2 Plot shows the fit of the observed data to a second order polynomial in energy

3. **Relationship between bandgap and post-temperatures compared with other determined or measured parameters**

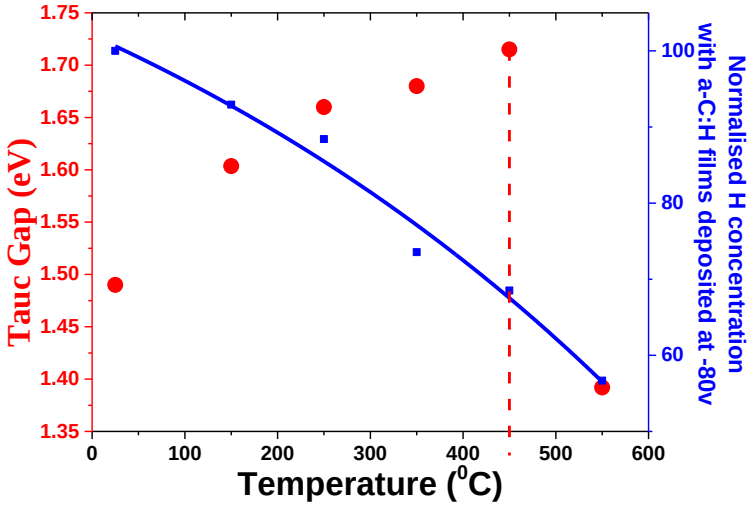

Fig.S3 The relationship between the hydrogen content in the a-C:H films and the bandgap at various post-annealing temperatures.

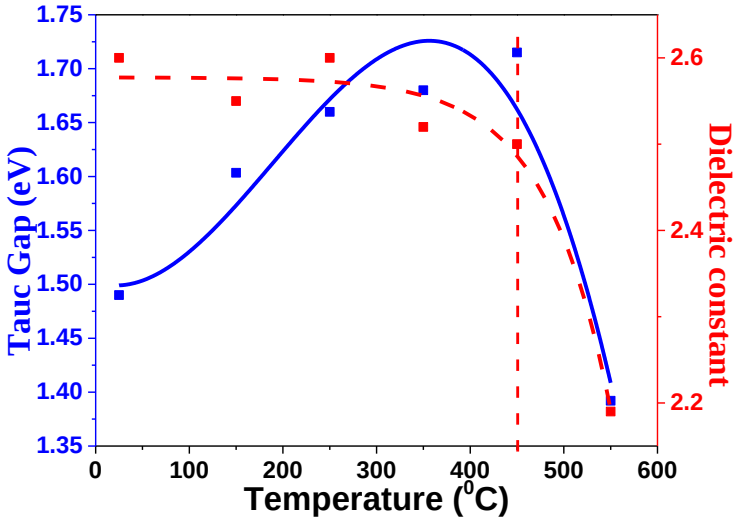

Fig.S4 Variation of Dielectric constant with Bandgap for a-C:H against annealing temperatures

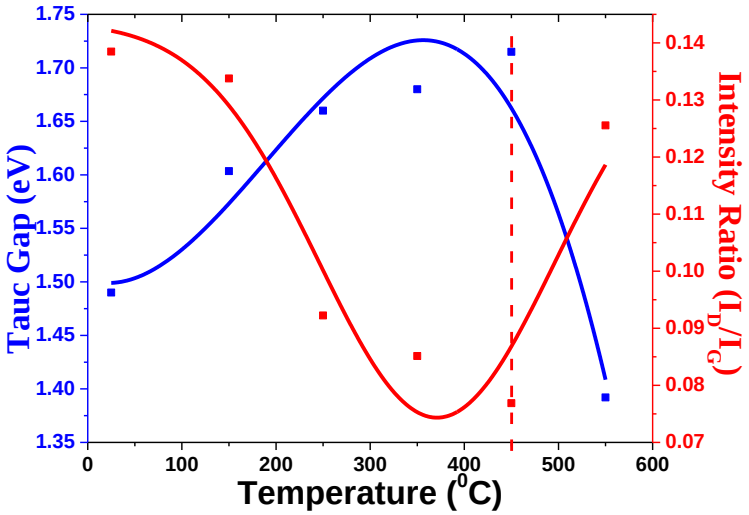

Fig.S5 Variation of I_D/I_G ratio with Bandgap for a-C:H against annealing temperatures. sp^2 clusters in a-C:H film control the Bandgap of the film that is good to describe the relationship between I_D/I_G ratio and the Bandgap**Error! Reference source not found.**.

4. Histogram of two terminal memory devices

In order to confirm the C-V characterisation results for the MIS structures with and without SeNPs, measurements were carried out on 12 reference devices and 12 MIS devices containing SeNPs. The flat band voltage shift was calculated, and a statistical analysis of the data was carried out to verify the observations, as shown in Fig.S5. The results confirm that

the flat band voltage derived from the C-V curve is similar with minimal deviation in the obtained values.

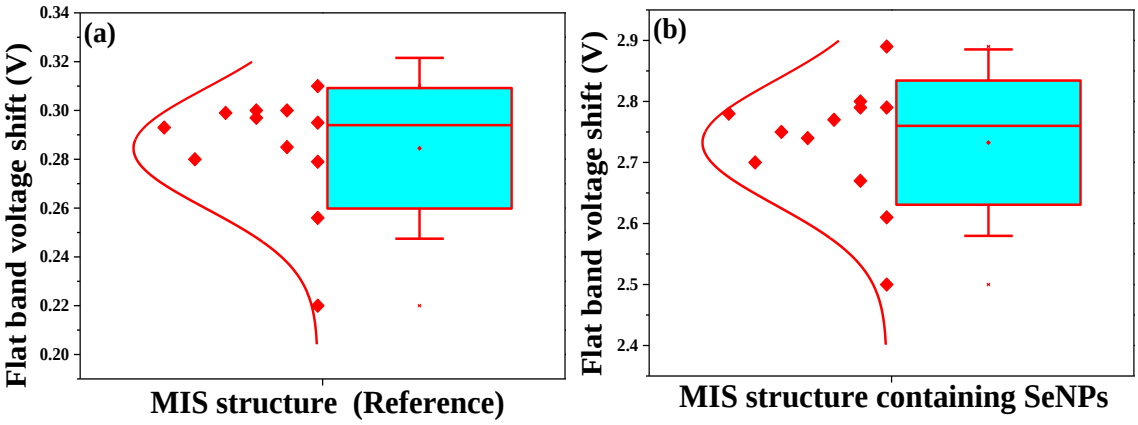

Fig.S5 Histogram distribution and box chart plot of the calculated flat band voltage shift of several devices: (a) 12 reference devices and (c) 12 memory devices with SeNPs.